INDIAN JOURNAL OF SCIENCE AND TECHNOLOGY

RESEARCH ARTICLE

OPEN ACCESS

Received: 01-06-2023

Accepted: 08-09-2023

Published: 17-10-2023

Citation: Praveendaniel M, Selvan PRA, Doss DPS (2023) Improved Optical, Photocatalytic, Electrical, And Antimicrobial Properties of Tio$_2$ Doped with Phosphomolybdic Acid Composites . Indian Journal of Science and Technology 16(38): 3267-3282. https://doi.org/10.17485/IJST/v16i38.1441

* **Corresponding author**.

rajesh.chem@stjohnscollege.edu

Funding: None

Competing Interests: None

Copyright: © 2023 Praveendaniel et al. This is an open access article distributed under the terms of the Creative Commons Attribution License, which permits unrestricted use, distribution, and reproduction in any medium, provided the original author and source are credited.

Published By Indian Society for Education and Environment (iSee)

ISSN
Print: 0974-6846
Electronic: 0974-5645

Improved Optical, Photocatalytic, Electrical, And Antimicrobial Properties of Tio$_2$ Doped with Phosphomolybdic Acid Composites

M Praveendaniel[1], P Rajesh Anantha Selvan[2]*, D Paramanantha Swami Doss[3]

1 Research scholar (Reg.No-20111272031005), Department of Chemistry, St. John's College, Affiliated to Manonmaniam Sundaranar University, Palayamkottai, Tirunelveli, Tamil Nadu, India

2 Assistant Professor, Department of Chemistry, St. John's College, Affiliated to Manonmaniam Sundaranar University, Palayamkottai, Tirunelveli,, Tamil Nadu, India

3 Assistant Professor, Department of Zoology, St. John's College, St. John's College, Affiliated to Manonmaniam Sundaranar University, Palayamkottai, Tirunelveli, Tamil Nadu, India

Abstract

Objectives: To synthesize a TiO$_2$-phosphomolybdic acid composite by sonication method. The above prepared samples were characterized and study the application. **Method:** The above prepared composites were characterized by UV-Visible, FTIR, XRD, EDAX and SEM studies. Also, the applications studies such as, photocatalytic activities, antimicrobial activities and electrical conductivities. **Findings:** The UV-Visible and FTIR shows that there is a strong interaction between TiO$_2$ and the dopant, phosphomolybdic acid. XRD and SEM showed a decrease in particle size and uniform distribution of dopant, phosphomolybdic acid into the TiO$_2$ matrix. The composite exhibited excellent photo-catalytic activity, with a degradation of MB at a rate of 99.58% with in 180min. The composites also had good antimicrobial activity with an inhibition rate 99%. The composites had good electrical conductivity with a conductivity of 100s/cm. **Novelty:** The light sensitizer functionality of TiO$_2$ and heterogeneous catalysis of phosphomolybdic acid, PMA have been combined in the composites.

Keywords: Composite; TiO$_2$ Phosphomolybdic Acid; Photocatalytic Activity; *Streptococcus pyogenes*; Dielectric Constant

1 Introduction

Titanium dioxide (TiO$_2$) composites are one of the most widely used materials in various fields due to their excellent physical and chemical properties. In recent years, TiO$_2$ composite materials have been studied extensively because of their potential applications in various fields, ranging from automotive and aerospace industries to medical, environmental, and energy applications. TiO$_2$ composites have been used in various forms including powder, nanoparticles, thin films, and nano-fibers.

They also have a unique combination of properties such as strong electrical conductivity, high thermal stability, and strong mechanical strength. In addition, they possess low-cost production which makes them suitable for industrial applications [1,2].

Phosphomolybdic acid is a widely used as homogeneous and heterogenous catalyst. The photocatalytic activity, electrical conductivity, and optical properties of the composite can be improved by doping TiO_2 with phosphomolybdic acid and lead to reducing the recombination of electron-hole pairs, enhanced the stability, catalytic activity, and increasing the adsorption capacity of the composite [3].

TiO_2-phosphomolybdic acid composite is a novel photocatalyst with enhanced photocatalytic activity [4], which, due to its unique structure. Its activity results from the presence of the two components, TiO_2 and phosphomolybdic acid. The combination of TiO_2 and phosphomolybdic acid results in unique interactions at the nano-level that boost the photocatalytic activity and enhance its activity for a broad range of industrial and environmental applications. In addition to its improved photocatalytic activity [5], TiO_2 doped with phosphomolybdic acid also exhibits other enhanced properties, such as increased electrical conductivity, improved mechanical strength, and better thermal stability. These properties make TiO_2-phosphomolybdic acid composite a promising material for a variety of applications.

TiO_2-phosphomolybdic acid composite is a material that is also used in antibacterial applications. This composite material has been found to possess a range of antibacterial properties when tested against various bacteria. The disc diffusion method of Streptococcus pyogenes is a commonly used method to evaluate the antibacterial activity of a material [6]. In this method, a disc of the composite material is placed on a plate of agar containing a bacterial culture. After a period of incubation, a zone of inhibition is observed around the disc, indicating the antibacterial effect of the composite material [7].

Composites were characterized by UV-DRS, FT-IR, XRD, and SEM-EDAX techniques. The optical property of these samples were investigated by UV-Vis Kubelka-Munk absorption. Measurements of the frequency-dependent conductivity of all the samples were performed using a Precision LCR Meter [Agilent 4284A] over a temperature range of 303 to 393 K and a frequency range of 100 Hz to 1 MHz. The results of the conductivity measurements were used to determine the electrical properties of the samples and to understand the effect of temperature and frequency on the conductivity. The photocatalytic degradation efficiency of doped composites were investigated by the photodegradation of Methylene Blue [MB] solution under visible light illumination. Furtherly, the effect of initial ion concentration, catalyst loading, and pH with irradiation time had been also studied. TiO_2-PMA composites were experimented with to find their antimicrobial activity against various bacterial species like Streptococcus pyogenes. Keeping application aspects of TiO_2-PMA composites in view, the present study has focused on photocatalytic and antimicrobial activity. Composites due to their unique physic-chemical and biological properties could have far-reaching industrial and microbial applications.

2 Methodology

The procedures for the synthesis of TiO_2 composite and TiO_2-doped Phosphomolybdic acid composites were briefly summarized below. The chemicals used in this study were all commercially available. TiO_2 was obtained from Loba Chemicals, HCl and NaOH pellets from Spectrum Chemicals, and phosphomolybdic acid from SRL Pvt. Ltd. Methylene blue dye was purchased from Himedia Ltd. All the reagents used in this study were of analytical grade

2.1 Synthesis of TiO2-Phosphomolybdic acid composites

The synthesis of TiO_2-doped with phosphomolybdic acid composites were carried out by sonication method. The sonication method was a simple and efficient way to synthesize TiO_2 composites. The sonication process helps to disperse the TiO_2 particles evenly in the solution, which results in a more uniform composite. The different concentrations of phosphomolybdic acid were used to study the effect of doping on the properties of the composites. 1 g of TiO_2 suspended in 50 mL of water in 250mL beaker and was sonicated for 60 minutes. The above sonication process was repeated with various concentrations of dopant phosphomolybdic acid (0.01 M, 0.001 M, 0.05 M, and 0.005 M) to prepare samples 2, 3, 4, and 5, respectively. After the sonication step, the suspensions were centrifuged to separate the precipitates from the supernatant. The precipitates were then dried in an oven at 110°C for 24 hours. The dried precipitates were ground into powder and stored for further study.

2.2 Characterization Techniques

The composites were commonly characterized by UV-DRS absorption spectroscopy and Fourier Transform Infra-Red (FTIR) spectroscopy. Their size, purity, morphology, and shape were found by using advanced techniques such as Powder X-ray Diffraction [PXRD], Scanning electron Microscopy (SEM-EDX), and Elemental analysis Mapping. Moreover, photodegradation, electrical and antimicrobial activity of composites were to be found.

2.2.1 UV DRS visible absorption spectroscopy

UV absorption of the synthesized composites had been carried out by using a JascoV-600 UV-Vis spectrometer, in the wavelength range 200-800 nm with a 1000 mm quartz cell. The spectrum was plotted as wavelength on X-axis and absorbance on the Y-axis.

Band gap energy can be done by applying the Tauc plot method, which involves plotting the absorbance (αhv)2 against the energy of the incident light (eV). The equation is

$$E = (\alpha hv)^2 \left(eVcm^{-1}\right)^2 vs \text{ Energy } (eV) \tag{1}$$

The Tauc plot is based on the relationship between the absorption coefficient α and the photon energy hν. This relationship is described by the following equation is

$$\alpha hv = A(hv - Eg)^n \tag{2}$$

where A is a constant, Eg is the band gap energy, and n is a parameter that depends on the material [7]. This equation states that when the photon energy is equal to the band gap energy, the absorption coefficient will be zero.

The Urbach energy method is based on the fact that the absorption coefficient of a material is exponentially dependent on the energy of the incident light. In this method, the Urbach energy (ΔE) is determined by fitting an exponential curve to the absorption spectrum of the material. The UV-Vis spectra of the pure TiO_2 and TiO_2 doped phosphomolybdic acid composites were measured in the range of 200-800 nm. The sample of the absorption spectra was obtained by plotting the absorbance (A) against the wavelength (λ).

2.2.2 Fourier Transform Infra-Red Spectroscopy

This technique was a very powerful technique that uses electromagnetic radiation in the infrared region for the determination and identification of molecular structures, in which FTIR spectra using model 8400S Shimadzu the electronic spectra Jasco 550 double beam spectrophotometer was used.

2.2.3 Powder X-ray diffraction

The particle size, purity, nature of the compound crystalline phase, and planes can be evaluated by using PXRD. Every single phase exhibits peak at different 2θ values. The 2θ values can interpret the exact phase of the sample. X-ray diffraction (PXRD) studies were carried out for the TiO_2-doped Phosphomolybdic acid composites by using a Philips powder X-ray diffractometer Model PW1710. The PXRD patterns were recorded in the 2θ range of 10º-80º with a step width of 0.02º and steps time of 1.25 sec using Cu Kα radiation, λ=1.5406 Å.

2.2.4 Scanning Electron Microscopy

SEM of TiO_2 doped Phosphomolybdic acid composites was carried out by using scanning electron microscopy SEM model TESCAN'S VEGAS-3 operating at 20kV.

2.3 Photocatalytic & Degradation studies

The photocatalytic degradation of Methylene Blue was carried out by using an inner radiation-type photocatalytic reactor. Dye solutions and the photocatalyst were aerated for 30 minutes to reach equilibrium before being placed in the reaction chamber and subjected to irradiation at 365 nm for 3h. Samples of the dye solution were taken at intervals of 10, 20, 30, 40, 50, 60, 120, and 180 minutes and their degradations were measured by using an Optical Density in UV-vis spectrophotometer. The percentage of degradation efficiency (η) was calculated by comparing the initial concentration (C_o) of Methylene Blue with the concentration (C_t) after a certain period (t). The equation used for the measurement was as follows:

$$\eta = \frac{(C_t - C_o)}{C_t \text{X} 100} \tag{3}$$

These experiments were conducted to measure the effect of initial concentration, catalyst loading pH variation, and irradiation to use had been studied.

2.4 Electrical conductivity of TiO_2 -PMA composites

The sample used for electrical conductivity was taken in a mortar and ground to form a powder. Then, 10% weight of polyvinyl alcohol was added as a binder to the powder. The powder was pressed into discs of 11 mm diameter and 3 mm thickness by applying a pressure of 260 MPa in a hydraulic press at room temperature. The resulting pellets had a uniform shape and size.

By using Two Probe methods, (AC with DC), the electrical conductivity of TiO_2 and TiO_2 doped phosphomolybdic acid composites had been taken. A Precision LCR Meter (Agilent 4284A) was used to measure the electrical conductivity of the samples within a temperature range of 303 to 393 K and a frequency range of 100 Hz to 1 MHz. Each sample was placed between two blocking electrodes with a diameter of 2.5 cm under spring pressure. This method was used to measure more accurate and detailed measurements of the conductivity of composites. Eventually, the two-probe method was a reliable and accurate method for measuring the electrical conductivity of TiO_2 and TiO_2-doped phosphomolybdic acid composites.

The AC conductivity was determined by using equation

$$\varepsilon_r = \frac{2\pi F cd}{A \tan \delta} \tag{4}$$

The dielectric constant ε_r was calculated by multiplying the capacitance c, distance d, and area A of the sample together, where the capacitance is determined by the frequency F of the signal and the loss tangent [tan δ]. The dielectric constant was a measure of the ability of the material to store energy in an electric field, while the loss tangent is a measure of the energy lost to heat.

The two-probe method was a reliable and versatile technique for measuring the dielectric constant of TiO_2 and TiO_{2-}doped phosphomolybdic acid (0.05M) composites. The procedure for measuring the dielectric constant of these composites using the two-probe method begins with the preparation of the sample. The plates were then connected to a two-probe apparatus, which consists of two metal plates separated by a dielectric material. A voltage was applied across the two probes and the capacitance of the sample and reference materials was measured. The area of the plates was also measured.

The dielectric constant was obtained from the following equation [(8)].

$$\varepsilon_r = \frac{cd}{A\varepsilon_o} \tag{5}$$

Where c is the measured capacitance of the sample composite, d is the distance between the two plates, A is the area of the plates, and ε_o is the permittivity of free space.

The dielectric loss [tanδ] was calculated using the following equation [(9)].

$$\tan \delta = \frac{\varepsilon_r}{\varepsilon_o} \tag{6}$$

The two-probe method was used to measure the dielectric loss of pure TiO_2 and TiO_2-doped phosphomolybdic acid (0.05M) composite . The method uses the equation [(6)], where ε_r is the relative dielectric constant and ε_o is the permittivity of free space.

2.5 Antimicrobial Activity of Composites

Bacterial strain preparation of Streptococcus pyogenes [MTCC 442] was acquired from the HiMedia Laboratories Pvt. Ltd. Mumbai, India. All the bacterial strains were cultured in the liquid medium, Mueller Hinton broth (M-H Broth) [HiMedia, Mumbai, India] at 33ºC for 2hrs with 200rpm stirring. The antimicrobial activity of TiO_2-doped phosphomolybdic acid composites was evaluated by the standard disk diffusion method. After incubating TiO_2 composite for 48hrs, bacterial suspensions of Streptococcus pyogenes were daubed on separate Nutrient Agar plates by L-rod. Whatman filter paper (No.1) and discs of 20 mm diameter were dividedly infused with a 20 μL solution of TiO_2 doped phosphomolybdic acid composite in dimethyl sulfoxide (DMSO). The discs were vaporized and impregnated on the plates. Antibiotics of Amoxicillin & Potassium Clavulanate 20 μL of 20 mg/mL solution were used as a positive control against fungus and bacteria to stop the bacterial growth respectively. Also, DMSO assisted as the negative control. Bacterial cultures were incubated at the temperature of 37^{o}C, while the fungus was incubated at the temperature of 33ºC for 48 hrs. The diameter activity zones of inhibition ring formation, growth in bacteria, and composites were examined.

3 Results and Discussion

3.1 UV-Vis spectra analysis

The UV-Vis spectrum of the above-prepared composite samples were recorded and the results were shown in Figure 1. The pure TiO_2 sample showed a strong absorption peak at 350 nm. Sample 2 acquired a slight increase in the absorbance at 356

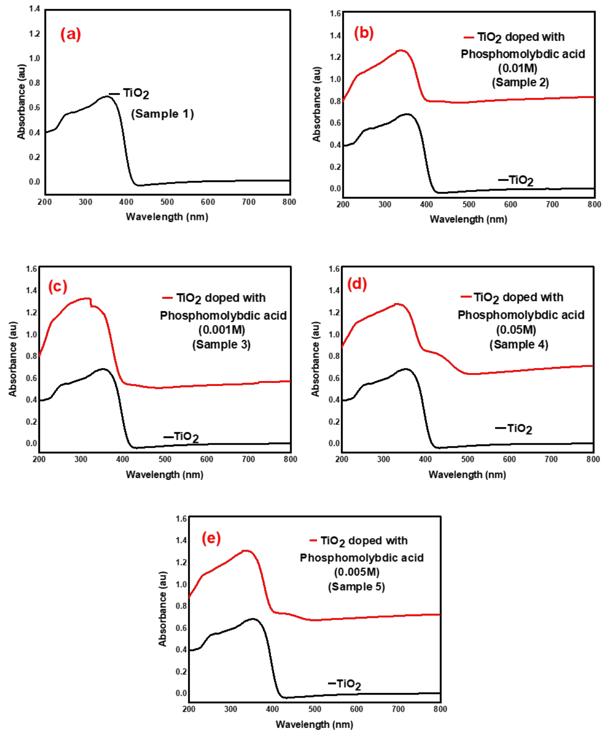

Fig 1. UV-Visible spectrum of TiO_2 and TiO_2 doped with Phosphomolybdic acid composite

nm, indicating the presence of the dopant. Sample 3 obtained a further decrease in absorbance, indicating an even lower concentration of phosphomolybdic acid. Sample 4 showed a higher absorbance at 360 nm indicating a higher concentration of phosphomolybdic acid. Sample 5 showed a slight decrease in the absorbance at 356 nm, indicating a lower concentration of phosphomolybdic acid [(10)].The results indicate that the addition of phosphomolybdic acid to TiO_2 increases the absorbance in the range of 354nm to 360nm. The addition of phosphomolybdic acid increases the stability of the TiO_2 composite , making it more suitable to be used in photocatalytic applications.

3.2 Determination of Bandgap Energy

TiO_2 is a widely used semiconductor in the field of optoelectronics due to its unique optical properties. By analyzing the UV-vis spectra of pure TiO_2 and TiO_2 doped with phosphomolybdic acid composites in different concentrations (0.01M, 0.001M, 0.05M, and 0.005M), the band gap energy can be determined [(11)].

The band gap energy of TiO_2 and its composites were shown in Figure 2 and Table 1. The UV-vis spectra of the pure TiO_2 reached an absorption peak at 3.2 eV and the absorbance increased rapidly with a further decrease in energy. The TiO_2 composites maintained a similar pattern of absorbance for pure TiO_2 however, the absorbance is lower due to the presence of the dopant. The band gap energies of the TiO_2 doped with phosphomolybdic acid composites of 0.01M, 0.001M, 0.05M, and 0.005M were 2.78 eV, 2.73 eV, 2.55 eV, and 2.42 eV respectively. These values indicate that the band gap energy of TiO_2 decreases with the increased concentration of the dopant. These results showed that phosphomolybdic acid dopants can effectively reduce the band gap energy of TiO_2 composites.

3.3 Determination of Urbach Energy

The UV-Vis spectra of pure TiO_2, and TiO_2 doped with phosphomolybdic acid concentrations of 0.01M, 0.001M, 0.05M, and 0.005M were analyzed by using the Urbach energy method. This analysis is a useful tool for investigating the optical properties of materials and characterizing their band gap structures. The spectra showed strong absorption peak in the UV region. The results exhibited that the Urbach energy of the pure TiO_2 sample was 0.90 eV. The value was slightly lower than the TiO_2-doped phosphomolybdic acid composites, (Table 1). Which ranged from 0.90 eV to 0.30 eV, depending on the concentration of the

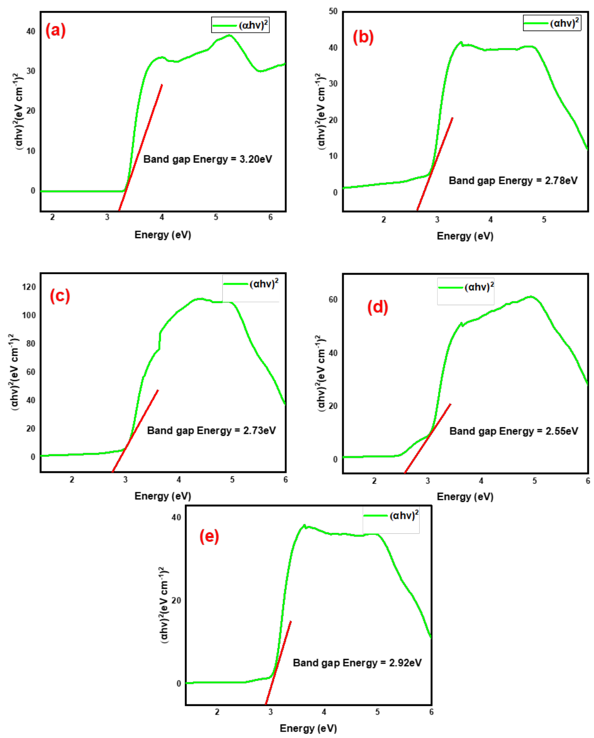

Fig 2. Band gap and Urbach energy of TiO_2 and TiO_2 doped with Phosphomolybdic acid composite

Table 1. V-DRS using Band gap and Urbach Energy.

No	Sample	UV-Vis peaks (nm)	Band gap Energy (eV)	Urbach Energy (meV)
1	**TiO_2**	350	3.20	0.93
2	**Doped Sample (0.01M)**	356	2.78	0.39
3	**Doped Sample (0.001M)**	334	2.73	0.30
4	**Doped Sample (0.05M)**	360	2.55	0.64
5	**Doped Sample (0.005M)**	356	2.92	0.50

doping agent. Eventually, the doping of phosphomolybdic acid into the TiO_2 had a significant effect on their optical properties, resulting in a lower Urbach energy [12].

3.4 FTIR Analysis

Figure 4 shows the FTIR analysis of sample 1 pure TiO_2. The absorption bands are 3408 cm^{-1} (asymmetric stretching of Ti-O), 2917 cm^{-1} (symmetric stretching of Ti-O), 1615 cm^{-1} (bending of Ti-O), 1372 cm^{-1} (bending of O-Ti-O), and 616 cm^{-1} (Ti-O stretching). These bands are characteristic of pure TiO_2. Sample 2 shows the absorption bands at 2934, 2379, 1641, 1380, and 679 cm^{-1} correspond to the characteristic peaks for TiO_2 and phosphomolybdic acid. The bands at 2934 cm^{-1} is due to the Ti-O stretching vibration in TiO_2, while the two new bands at 2379 and 1641 cm^{-1} are due to the P-O and Mo-O stretching vibrations in phosphomolybdic acid. The bands at 1380 cm^{-1} is due to the Mo-O-Mo bending vibration in phosphomolybdic acid, and the bands at 679 cm^{-1} is due to the Ti-O bending vibration in TiO_2. Sample 3 shows the absorption bands at 2888, 2367, 1636, 1359, and 675 cm^{-1} are similar spectrum to Sample 2, but the peaks are slightly weaker. This is because the concentration of phosphomolybdic acid is lower in Sample 3. Sample 4 shows the bands at 2926, 2379, 1653, 1385, and 657 cm^{-1} are spectrum with more pronounced bands than Samples 2 and 3. This is because the concentration of phosphomolybdic acid is higher in Sample 4. Sample 5 shows the absorption bands at 2850, 2388, 1641, 1372, and 696 cm^{-1} are spectrum with a slightly different shape than the other samples. This is because the concentration of phosphomolybdic acid is very low in Sample 5, and the peaks

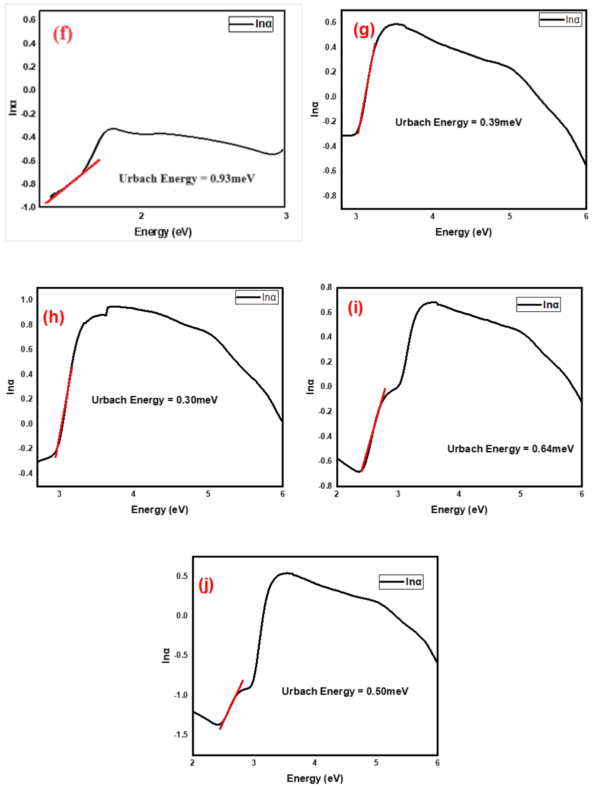

Fig 3. Band gap and Urbachenergy of TiO_2 and TiO_2 doped with Phosphomolybdic acidcomposite (Continuous)

are more spread out.

The results of the FTIR analysis show for the samples 2 to 5 show that the doping of TiO_2 with phosphomolybdic acid causes a shift in the wavenumbers of the bands. This shift is due to the interaction between the TiO_2 and the phosphomolybdic acid molecules. The higher the concentration of phosphomolybdic acid, the larger the shift in the wavenumbers of the bands[13].

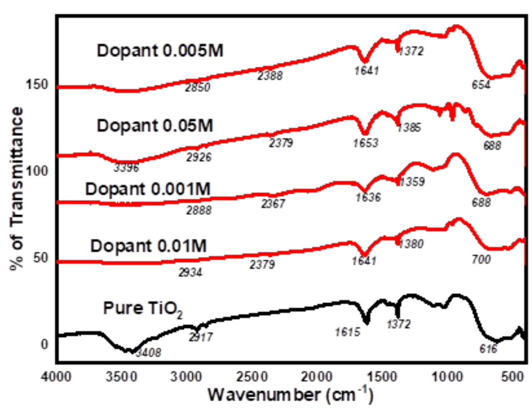

Fig 4. FTIR spectra of TiO_2doped phosphomolybdic acid composites

3.5 XRD Analysis and W-H Plot

The XRD graphs of Pure TiO_2 and TiO_2 doped with Phosphomolybdic acid composites with concentrations 0.01M, 0.001M, 0.05M, and 0.005M were shown in Figure 4. The XRD pattern of pure TiO_2 (JCPDS File No. 89-6975) is (110), (101), (111), (210), (211), (220), (002), and (311) planes and corresponding 2θ angles were 27.14°, 35.79°, 38.92°, 40.96°, 43.77°, 54.07°, 56.37°, 62.52°, 63.81°, and 68.77°, respectively. It can be seen that the peak intensity of the (111) plane was the highest among all the frequencies. This was for a tetragonal structure. The sharpness of the peak indicates that the TiO_2 sample was crystalline [14]. The XRD results of TiO_2 doped with phosphomolybdic acid composite (0.01M, 0.05M, 0.001M, and 0.005M] were also presented here. The XRD pattern of the samples is compared with JCPDS File No. 39-0026 shown in Figure 5. The main peak of the XRD pattern have the 2θ angles 27.21°, 34.50°, 36.14°, 54.04°, 56.32°, and 68.71°. From the XRD pattern, it can be seen that the peak intensity of the (100) plane was the maximum among all the frequencies. This was typical of a monoclinic structure. The sharpness of the peak indicates that the samples were more crystalline. The XRD results show that the doping of phosphomolybdic acid slightly affects the crystallinity of the TiO_2. The presence of the dopant can be confirmed through the shift in the peak positions. The peak positions of the phosphomolybdic acid composite samples were shifted away from the peak positions of the pure TiO_2 sample. The XRD results of this study were in agreement with the literature, confirming the successful incorporation of PMA into TiO_2 and the formation of composites with improved properties. The information about the particle size of TiO_2 doped with phosphomolybdic acid composites had been obtained from the following Scherrer relations.

$$D = \frac{0.94\lambda}{\beta \cos\theta} \tag{2}$$

where D is the average particle size, λ is the wavelength of the incident X-ray is 1.5418Å, β is the full widths half maximum FWHM of the X-ray, and θ is the diffraction peak position in the diffractograms. The average particle size is given in Table 2.

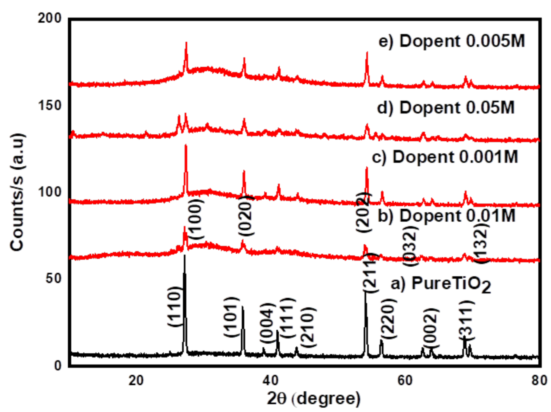

Fig 5. XRD spectrum of Phosphomolybdic acid doped TiO_2 composites

Table 2. W-H method for TiO_2-PMA composite

Composites	Parameters		Peak Position	FWHM	Intercept	Crystallite Size	Slope	Micro strain $(\varepsilon)X10^{-3}$	d-spacing (Å)	Average d-spacing (Å)
	K	λ(Å)	2θ (°)	β (°)	c=kλ/D	D(nm)	m		d_{hkl} $=\lambda/(2\sin\theta)$	
Pure TiO_2	0.94	1.54	27.14	0.2775	0.0037	29.63	0.0004	0.48	3.28	1.99
TiO_2 +PMA 0.01M	0.94	1.54	27.21	0.4786	0.0088	10.56	0.0006	0.65	3.27	2.05
TiO_2 +PMA 0.001M	0.94	1.54	27.30	0.7099	0.0037	11.92	0.0004	0.40	3.26	1.99
TiO_2 +PMA 0.05M	0.94	1.54	10.78	0.0086	0.0307	100	0.0040	4.00	8.19	3.02
TiO_2 +PMA 0.005M	0.94	1.54	27.58	8.8978	0.0097	15.77	0.0041	4.17	3.23	2.21

The W-H plot was used to analyze the XRD results of pure TiO_2 and TiO_2 doped with phosphomolybdic acid composite having concentrations 0.01M, 0.05M, 0.001M, and 0.005M shown in Table 2. The W-H plot is a valuable tool in XRD analysis and can provide valuable information about the structure of a material. The d-spacing results show that the addition of phosphomolybdic acid composite in the TiO_2 samples led to slight changes in the d-spacing. The results also show that the d-spacing of the samples increased with an increase in the concentration of phosphomolybdic acid composite . The results indicate that the addition of phosphomolybdic acid in the TiO_2 samples caused a slight increase in the d-spacing of the samples.

3.6 SEM-EDAX Analysis

The SEM images of pure TiO_2 and TiO_2 doped with phosphomolybdic acid at various concentrations of 0.01M, 0.001M, 0.05M, and 0.005M were shown in Figure 6. In the SEM images, the particles are spherical with a smooth surface. The particles of SEM images have a uniform size distribution, with an average particle size ranging from 500nm. The surface of the particles was relatively smooth, with no visible large pores or cracks. At the concentration of PMA in sample 2 (0.01M) the particles were larger and more densely packed, while in sample 3 [0.001M) they appear to be smaller and more scattered. As the concentration of PMA increases, the particles become more uniform in size and shape, with a higher density of particles. At a concentration of PMA in sample 4 (0.05M), the particles were about the larger size, but appear to be more tightly packed together. Finally, at a concentration of PMA in sample 5 (0.005M), the particles had a more uniform size and shape, with a higher density of particles. In every SEM image, the particles appear to be composed of a core of TiO_2 surrounded by a thin layer of phosphomolybdic acid. The thin layer of phosphomolybdic acid forms a protective coating around the TiO_2 core, which prevents the particles from clumping together and helps to preserve their spherical shape. The size and shape of the particles differ slightly depending on the concentration of the composites[15].

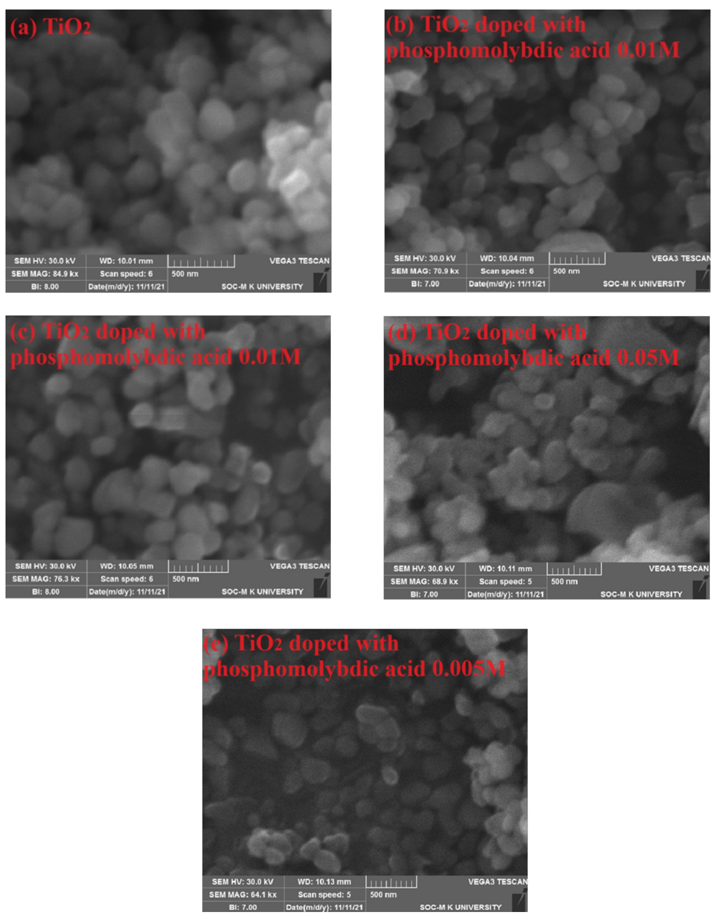

Fig 6. SEM & EDAX ofPure TiO_2 and TiO_2 doped with Phosphomolybdic acidcomposites, average diameter analysis

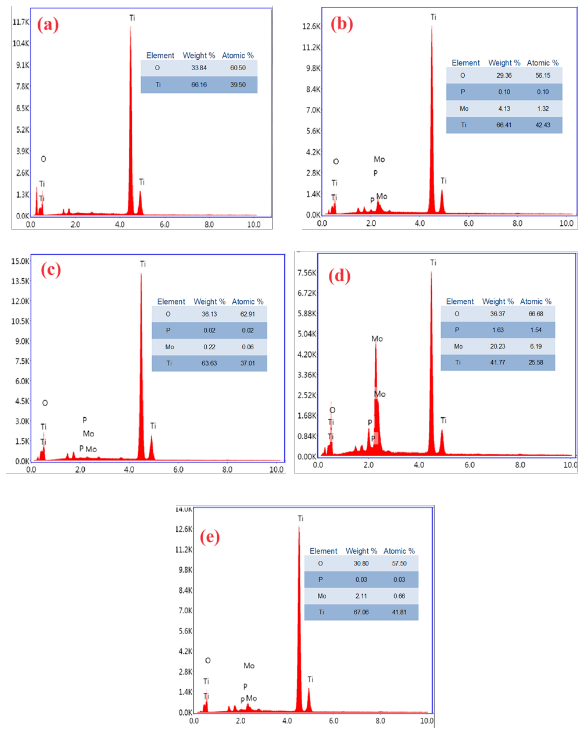

Fig 7. SEM & EDAX of Pure TiO_2 and TiO_2doped with Phosphomolybdic acid composites, average diameter analysis(Continuous)

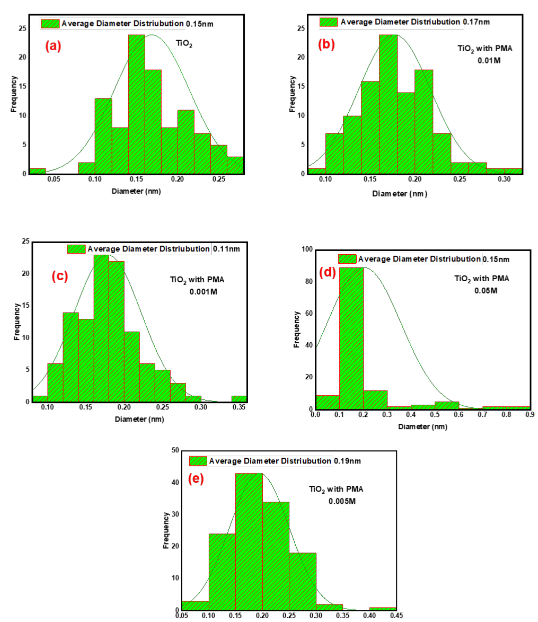

Fig 8. SEM & EDAX ofPure TiO_2 and TiO_2 doped with Phosphomolybdic acidcomposites, average diameter analysis (Continuous)

EDAX analysis had been used to examine the composite of pure TiO_2 and TiO_2 doped with phosphomolybdic acid. The results of the analysis reveal that the composite consists of titanium, oxygen, phosphorus, and molybdenum. The TiO_2 particles were found to be dispersed homogeneously. The phosphomolybdic acid was evenly distributed and successfully doped the TiO_2 particles. The presence of phosphorus and molybdenum confirms that the composite was composed of PMA materials, as intended.

3.7 Average Diameter Distribution analysis

ImageJ is a software application which is used for the analysis of digital images [16].It is useful for various applications, including the analysis of nanocomposites. This can be done by measuring the size, shape and distribution of the nanocomposites. In this study, ImageJ were used to analyze the Pure TiO_2 (0.15nm) and TiO_2-phosphomolybdic acid nanocomposites with different concentrations (0.01M, 0.001M, 0.05M and 0.005M). The results revealed that the mean particle size of the Pure TiO_2 nanocomposite were 0.15nm, The mean particle size of the various concentrations of TiO_2 doped with phosphomolybdic acid were 0.17, 0.11, 0.15 and 0.19 nm respectively. The number of particles and percentage of the area of every image were occupied by the nanocomposites which were increased by increasing the concentration of phosphomolybdic acid. The results obtained with ImageJ showed that the mean particle size of the nanocomposites had increased by increasing concentration of the phosphomolybdic acid. This suggests that the phosphomolybdic acid may be acting as a surfactant, increasing the surface area of the nanocomposites and their size. Furthermore, indicating that the nanocomposites were more densely packed.

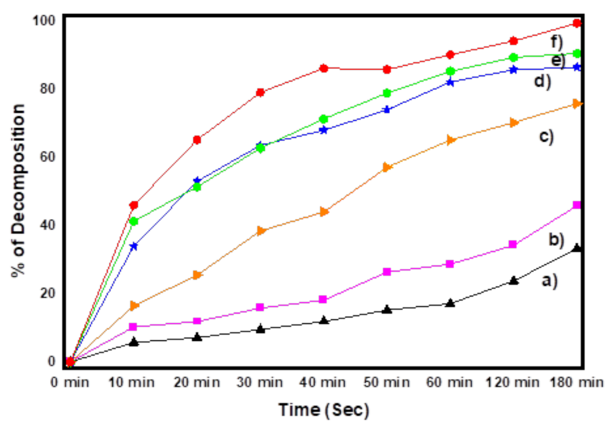

Fig 9. Phosphomolybdic acidphotocatalyst concentration variation, a) 10mg b) 20mg c) 50mg d) 100mg e) 125mg f) 150mg,n Condition: Methylene blue = 50mg/L; Temp = 33ºC; Without airflow and Photodegradation wavelength = 365nm, and O.D measured at λmax= 460 nm

3.8 Photocatalytic Studies

3.8.1 Photodegradation studies of methylene blue dye by TiO2-PMA without airflow

The photodegradation of methylene blue dye [17]was studied by using TiO_2 doped with phosphomolybdic acid as the catalyst. The initial concentration of the dye was 50mg/L and the catalyst dosage at 0.5g/L, without airflow. The wavelength used for photodegradation was 365 nm. The results of the study showed that a maximum of 99.58% degradation of the dye was achieved. The absence of airflow thus improved the photodegradation activity of the TiO_2 doped with phosphomolybdic acid composite.

3.8.2 Effect of pH on photocatalytic degradation of methylene blue

The photocatalytic degradation of methylene blue was studied at different pH values [18].A solution of methylene blue at a concentration of 50mg/L was mixed with 0.5g/L of the catalyst and exposed to UV radiation at 365nm. The pH was adjusted to 4, 6, and 8 by adding 0.1M of HCl and NaOH, after 60 minutes, the efficiency of degradation was found to be 98.82%, 77.46%, and 63.19%, respectively. The highest degradation efficiency was observed at pH 4, and the lowest at pH 6 and 8. Therefore, pH 4 is helpful to the maximum degradation of methylene blue. This was confirmed by the results obtained, with the highest degradation at pH 4. The results of this study indicate that pH plays an important role in the photocatalytic degradation of

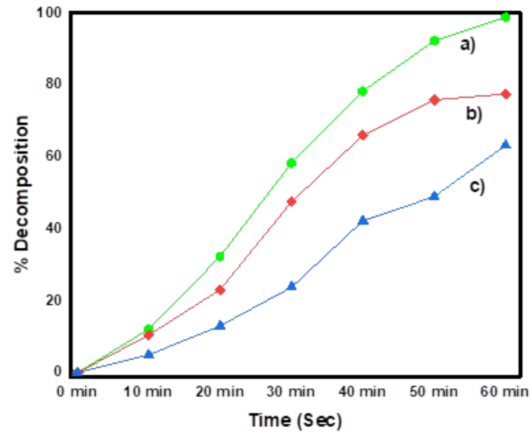

Fig 10. Effect of pH variation on photodegradation of methylene blue a) 4 b) 6 c) 8 Condition: Methylene blue = 50mg/L; Temp = 33ºC; catalyst dose = 0.5g/Land Photodegradation wavelength = 365nm

methylene blue. As the pH of the solution increases, the rate of degradation decreases. Thus, to obtain the best results, the pH of the solution should be adjusted to 4. This will provide the optimum pH conditions for the photocatalytic degradation of methylene blue.

3.8.3 Effect of demineralization of Methylene blue dye

Methylene blue is a dye, it was capable of absorbing a wide range of wavelengths, which allows it to be used for their demineralization and this can be done through photocatalysis. Photocatalysis involves the absorption of ultraviolet light by the dye, which results in the formation of reactive oxygen species that can oxidize the dye. In addition, the dye can also reduce the surface tension of the water, making it more conducive to complete demineralization [(19)]. The demineralization of Methylene blue dye was studied by subjecting it to optimized conditions. This included the concentration of dye at 50mg/L, catalyst dose of 0.5g/L, temperature 33ºC, pH=4, and UV wavelength of 365nm for the photodegradation. The results showed that the dye was able to be completely demineralized within 4 hours. This shows that the photocatalytic effect of methylene blue dye can be used to enhance the efficiency of existing water treatment technologies. It can be used to reduce the levels of pollutants and harmful bacteria in water and make it more suitable for drinking and other uses.

3.9 Electrical conductivity studies by Two probe Method

The electrical conductivity of both pure TiO_2 and TiO_2 doped with phosphomolybdic acid (0.05M) composite was measured by using two probe methods. The electrical conductivity of the pure TiO_2 sample was found that it was lower than that of the TiO_2 doped with phosphomolybdic acid (0.05M) composite sample. This difference in conductivity can be attributed to the doping of the sample with the phosphorus-molybdenum heteropoly acid, which acts as an electron donor, increasing the number of available charge carriers and electrical conductivity. The doping of the sample with the phosphorus-molybdenum heteropoly acid created a more ordered network, which also contributed to the increased electrical conductivity. The conductivity of the doped sample increased when the frequency was increased from 100 Hz to 1 MHz, indicating a frequency-dependent response. At high frequencies, the charge carriers had more time to move around and, if increased the electrical conductivity. The results obtained from this study demonstrate that the doping of TiO_2 with phosphomolybdic acid [0.05M] composite can significantly improve the electrical conductivity of the material. This comparison can be used to understand the differences in the electrical properties of the two materials and used to investigate their behavior further.

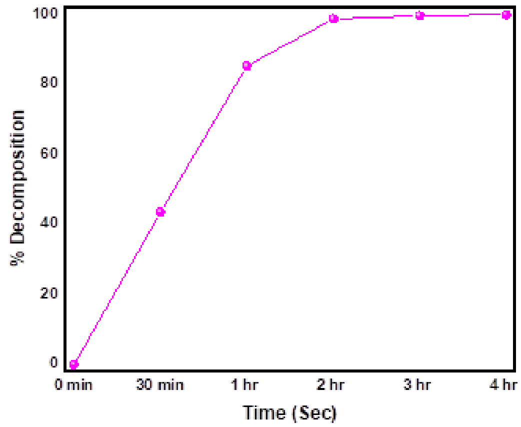

Fig 11. Effect ofdemineralization of Methylene blue dye Condition: Methylene blue = 50mg/L;Temp = 33ºC; catalyst dose = 0.5g/L and Photodegradation wavelength = 365nm

3.9.1 AC conductivity studies

The frequency-dependent AC conductivity [20] of TiO_2 and TiO_2 doped with Phosphomolybdic acid [0.05M] composites are shown in Figure 12.

The TiO_2 has a wide band-gap energy and an electrical insulator, when it is doped with phosphomolybdic acid, it exhibits increased electrical conduction. The increased electrical conduction of the doped TiO_2 composite existed due to the increased number of free charge carriers, which enables the material to store more energy. The dielectric constant and loss tangent of the doped TiO_2 composite was found to be higher than those of the pure TiO_2, showing that doping the material with phosphomolybdic acid improves its electrical properties. The increased electrical conduction of the doped TiO_2 composite could be used for various applications, such as electrodes and solar cells.

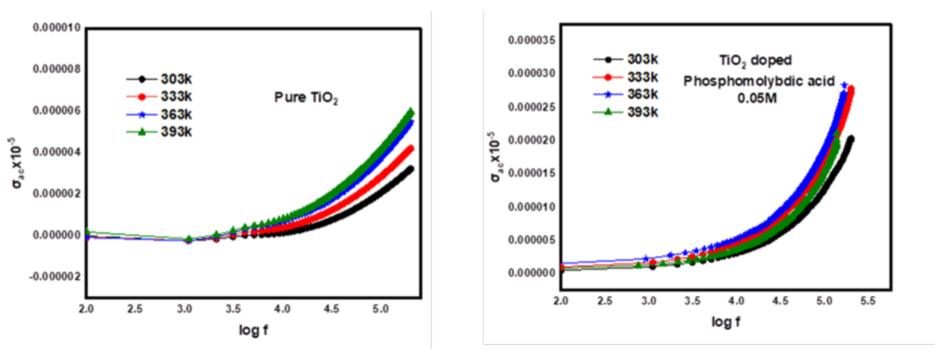

Fig 12. Frequency dependent AC of Pure TiO_2 and TiO_2 doped Phosphomolybdic acid (0.05M) composites at varying temperatures

In, Figure 13 the DC conductivity [21] of pure TiO_2 and TiO_2 doped with phosphomolybdic acid (0.05M) composites at a temperature of 35°C were given. It shows a linear relationship between voltage and current, with a saturation point at around 400V. At low voltage, the current is low and the resistance of the material is high. However, as the voltage increases, the current increases and the resistance of the material decreases. The saturation point was reached at 400V, where the resistance of the material was no longer changing with increasing voltage, and the current remains constant.DC Conductivity of Pure TiOand TiOcomposites

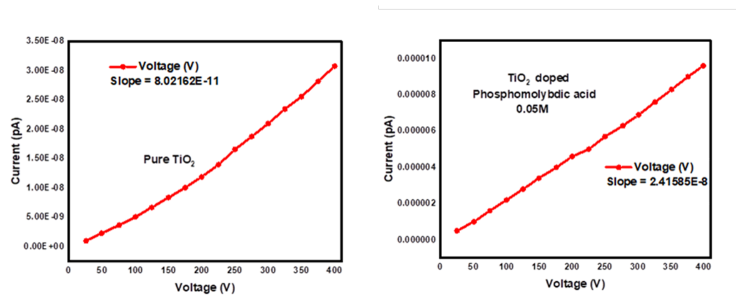

Fig 13. DC Conductivity of Pure TiO_2 and TiO_2 doped with Phosphomolybdic acid (0.05M) composites at varying temperatures

3.9.2 Dielectric studies

The results were shown in Figure 14, that the dielectric constant of the TiO_2 and TiO_2 doped phosphomolybdic acid [0.05M] composite was significantly higher than that of pure TiO_2. This was attributed to the presence of phosphomolybdic acid in the composites, which increases the dielectric constant of the material due to its polar nature. Additionally, it was found that the dielectric constant of the material increases with increasing doping concentration, indicating that the doping of phosphomolybdic acid can be used to tune the dielectric constant of the composites.Frequency dependent dielectric constant for Pure TiOcomposites at varying temperatures.

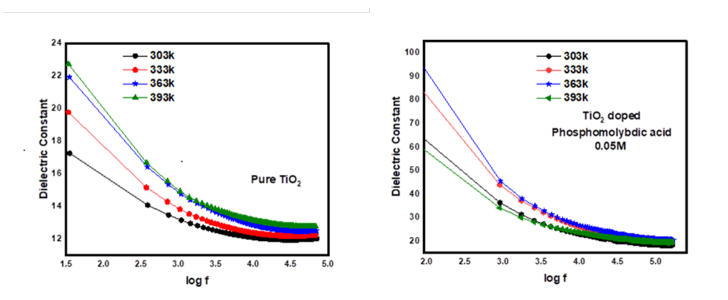

Fig 14. Frequency dependent dielectric constant for Pure TiO_2 and TiO_2 doped Phosphomolybdic acid (0.05M) composites at varying temperatures

In Figure 15 the results of the two-probe method showed that the dielectric loss of the TiO_2-doped phosphomolybdic acid composite was much higher than that of pure TiO_2. This indicates that the composite had much higher dielectric losses than pure TiO_2. The higher dielectric losses of the composite can be attributed to the doping of phosphomolybdic acid, which increased the dielectric constant of the material. The higher dielectric constant of the composite resulted in higher dielectric losses. This finding indicates that the two-probe method is an effective way to measure the dielectric loss of materials.

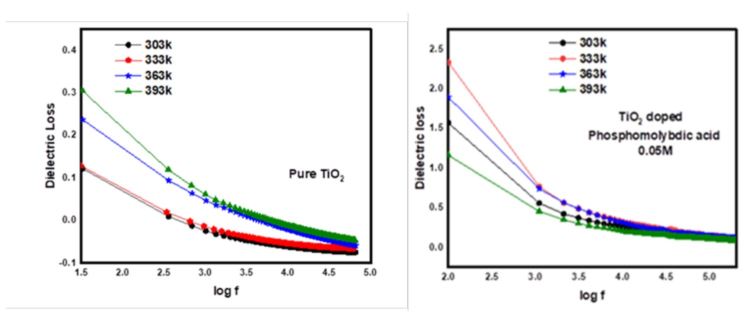

Fig 15. Frequency dependent Dielectric Loss for Pure TiO2 and TiO2 doped Phosphomolybdic acid (0.05M) composites at varying temperatures

3.10 Antimicrobial Activity of Disc Diffusion Method

The antibiotic combination of amoxicillin and potassium clavulanate has been widely used in the treatment of infections caused by Streptococcus pyogenes bacteria, a common cause of dental caries [22].To evaluate the antimicrobial activity of amoxicillin and potassium clavulanate, a disc diffusion method was employed by using a TiO_2–doped phosphomolybdic acid composite. The composite was dissolved in dimethylformamide and then applied to filter paper discs. These discs were then placed on the agar plates containing the Streptococcus pyogenes bacteria. The plates were then incubated for 48 hours at 37°C. After the incubation period, the inhibitory effect of the composite was assessed by measuring the diameter of the zone of inhibition around the paper discs. The results showed that the TiO_2-doped phosphomolybdic acid composite had a potent antimicrobial effect against Streptococcus pyogenes bacteria. The zone of inhibition around the discs containing the composite was significantly larger than that of the control discs, indicating that the composite was effective at inhibiting the growth of the bacteria. Moreover, the combination of amoxicillin and potassium clavulanate displayed a strong antimicrobial activity than the composite alone, indicating that the two antibiotics synergistically enhanced the antimicrobial activity of the composite. Overall, the disc diffusion method, using TiO_2-doped phosphomolybdic acid composite combined with amoxicillin and potassium clavulanate, demonstrated a potent antimicrobial effect against Streptococcus pyogenes bacteria. This suggests that the combination of these two antibiotics with the composite could be used as an effective treatment for infections caused by this particular bacteria [23].

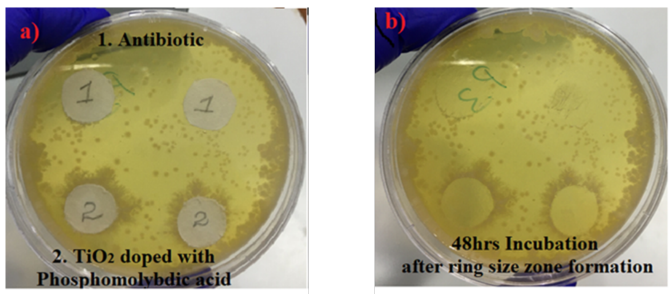

Fig 16. Anti mycobacterial activity TiO_2 doped phosphomolybdic acid composites

4 Conclusion

TiO_2-PMA composites, were synthesized by TiO_2 doped with various concentrations of phosphomolybdic acids by sonication method. UV-Vis and FTIR spectra revealed the strong interaction between TiO_2 and metal-heteropoly acid. The structural morphology of the composites was examined by SEM analysis. EDX analysis was used to confirm the purity of the samples and XRD showed that the composites were crystalline. Furthermore, the photocatalytic activity of the composites was evaluated, showing 99.58% degradation efficiency at pH 4, Condition**:** [Methylene blue] = 50mg/L, 3ºC; catalyst dose = 0.05M, without airflow and Photodegradation wavelength = 365nm. These results indicate that the light absorption of TiO_2 and the catalytic role of phosphomolybdic acid are intervened, allowing for enhancing photocatalytic activity. The composites were also found to have strong antibacterial activity, suggesting potential applications. Moreover, the composite exhibit temperature and frequency-dependent AC and DC conductivities. The enhanced photocatalytic activity, simple fabrication, electrical conductivity, and antibacterial activity of the TiO_2-phosphomolybdic acid composites render them a potential application material.

4.1 Acknowledgment

All the authors are thankful to the Department of Chemistry & Zoology, St. John's College, Palayamkottai. For providing necessary facilities to conduct the experiments.

References

1) Zalani M, Nazanin B, Kaleji BK, Mazinani. Synthesis and Characterisation of the Mesoporous ZnO-TiO2 Nanocomposite; Taguchi Optimisation and Photocatalytic Methylene Blue Degradation under Visible Light. *Materials Technology*. 2020;p. 281–289. Available from: https://doi.org/10.1080/10667857.2019.1678087.
2) Yimyai T, Crespy D, Pena-francesch A. Self-Healing Photochromic Elastomer Composites for Wearable UV-Sensors. *Advanced Functional Materials*. 2023;33(20). Available from: https://doi.org/10.1002/adfm.202213717.

3) Deng C, Lv Y, Sun M, Yaseen M, Li S, Wang L. Phosphomolybdic Acid Clusters and Carbon Nitride Coloading on Nh2-N-Rgo for Photocatalytic Oxidation Desulfurization. *Journal of SSRN*. 2023. Available from: http://dx.doi.org/10.2139/ssrn.4480880.
4) Sahoo D, Tyagi S, Agarwal S, Shakya J, Ali N, Yoo WJ, et al. Cost-Effective and Highly Efficient Manganese-Doped MoS₂ Nanosheets as Visible-Light-Driven Photocatalysts for Wastewater Treatment. *Langmuir*. 2023;39(20):7109–7121. Available from: https://doi.org/10.1021/acs.langmuir.3c00390.
5) Mahamud M, Taddesse AM, Bogale Y, Bezu Z. Zeolite supported CdS/TiO2/CeO2 composite: Synthesis, characterization and photocatalytic activity for methylene blue dye degradation. *Materials Research Bulletin*. 2023;161:112176. Available from: https://doi.org/10.1016/j.materresbull.2023.112176.
6) Yihui W, Sun Y, Liu S, Zhi L, Wang X. Preparation of Sono activated TiO2-DVDMS Nanocomposite for Enhanced Antibacterial Activity. *Ultrasonics Sonochemistry*. 2020. Available from: https://doi.org/10.1016/j.ultsonch.2020.104968.
7) Neha R, Chahal S, Chauhan A, Kumar P, Shukla R, Singh SK. Analysis of MgO Nanoparticles by Modified Scherer's Williamson-Hall and Size-Strain Method. *Materials Today: Proceedings*. 2019;p. 12–543. Available from: https://doi.org/10.1016/j.matpr.2019.03.096.
8) Weiwang W, Li S. Improvement of Dielectric Breakdown Performance by Surface Modification in Polyethylene/TiO2 Nanocomposites. *Materials*. 2019;12(20). Available from: https://doi.org/10.3390/ma12203346.
9) Arularasu M, Harb M, Sundaram R. . Available from: https://doi.org/10.1016/j.carbpol.2020.116868.
10) Zhilei S, Pichugin VF, Konishchev EKE, Syrtanov ME, Kudiiarov MS, N V, et al. Effect of Nitrogen-Doping and Post Annealing on Wettability and Band Gap Energy of TiO2 Thin Film. *Applied Surface Science*. 2020. Available from: https://doi.org/10.1016/j.apsusc.2019.144048.
11) Hana K, Zlamalova M, Tarabkova H, Jirkovsky J, Frank O, Kohout M, et al. Rutile TiO2 Thin Film Electrodes with Excellent Blocking Function and Optical Transparency. *Electrochimica Acta*. 2019;p. 321. Available from: https://doi.org/10.1016/j.electacta.2019.134685.
12) Lakshmi MS, Wabaidur SM, Alothman ZA, Johan MR, Ponnusamy VK, Dhanusuraman R. Phosphotungstic acid-Titania loaded polyaniline nanocomposite as efficient methanol electro-oxidation catalyst in fuel cells. *International Journal of Energy Research*. 2021;45(6):8243–8254. Available from: https://doi.org/10.1002/er.5950.
13) Basel AS, Amer W, Kandyel EE, Ayad MM. Enhanced dual catalytic activities of silver-polyaniline/titanium dioxide magnetic nanocomposite. 2020. Available from: https://doi.org/10.1016/j.jphotochem.2020.112423.
14) Saad A, Kareem YS, Mohammed MS. Catalytic-oxidative/adsorptive denitrogenation of model hydrocarbon fuels under ultrasonic field using magnetic reduced graphene oxide-based phosphomolybdic acid (PMo-Fe3O4/rGO). 2020. Available from: https://doi.org/10.1016/j.ultsonch.2020.105050.
15) Subhasis D, Satpati B, Bhattacharya TS, Bala T. Synthesis of Au–Ag Triangular Nanocomposite with Promising SERS Activity. 2020. Available from: https://doi.org/10.1016/j.nanoso.2020.100438.
16) Ali RM, Hadi M, Mirsadri SA. Synthesis of New Nanocomposite Based on Nanoceramic and Mono Substituted Polyoxometalate, PMo11Cd@MnFe2O4, with Superior Catalytic Activity for Oxidative Desulfurization of Real Fuel. *Applied Organometallic Chemistry*. 2020;34(10). Available from: https://doi.org/10.1002/aoc.5882.
17) Dali R, Sarker M, Uddin MN, Elias Z, Rahman. P-doped TiO2-MWCNTs nanocomposite thin films with enhanced photocatalytic activity under visible light exposure. *Cleaner Engineering and Technology*. 2022;6. Available from: https://doi.org/10.1016/j.clet.2021.100364.
18) Sankar KV, Ashok M. Significantly enhanced photo catalytic activities of PbBi2Nb2O9(Bulk)/TiO2(Nano) hetero structured composites for methylene blue dye degradation under visible light. *Materials Chemistry and Physics*. 2020;244:122659. Available from: https://doi.org/10.1016/j.matchemphys.2020.122659.
19) Lenny R, Kurniawan R, Prasetyo N, Sudiono S, Syoufian A. Copper-and-Nitrogen-Codoped Zirconium Titanate (Cu-N-ZrTiO4) as a Photocatalyst for Photo-Degradation of Methylene Blue under Visible-Light Irradiation. *Indonesian Journal of Chemistry*. 2023;(2):416–416. Available from: https://doi.org/10.22146/ijc.78908.
20) Sengwa RJ, Dhatarwal P. Polymer nanocomposites comprising PMMA matrix and ZnO, SnO2, and TiO2 nanofillers: A comparative study of structural, optical, and dielectric properties for multifunctional technological applications. *Optical Materials*. 2021;113:110837. Available from: https://doi.org/10.1016/j.optmat.2021.110837.
21) Ragab HM. Enhancement in optical, thermal and electrical properties of Polyvinyl pyrrolidone/ polyethylene oxide matrix-based nanocomposites for advanced flexible optoelectronic technologies considering nanoceramic zinc oxide/titanium dioxide filler. *Journal of Molecular Structure*. 2023;1275:134663. Available from: https://doi.org/10.1016/j.molstruc.2022.134663.
22) Schutte-Smith M, Erasmus E, Mogale RE, Marogoa N, Jayiya A, Visser HG. Using visible light to activate antiviral and antimicrobial properties of TiO2 nanoparticles in paints and coatings: focus on new developments for frequent-touch surfaces in hospitals. *Journal of Coatings Technology and Research*. 2023;20(3):789–817. Available from: https://doi.org/10.1007/s11998-022-00733-8.
23) Wysocka I, Kowalska E, Ryl J, Nowaczyk G, Zielińska-Jurek A. Morphology, Photocatalytic and Antimicrobial Properties of TiO2 Modified with Mono- and Bimetallic Copper, Platinum and Silver Nanoparticles. *Nanomaterials*. 2019;9(8):1129. Available from: https://doi.org/10.3390/nano9081129.